ICES Journal of Marine Science

ICES International Council for the Exploration of the Sea
CIEM Conseil International pour l'Exploration de la Mer

ICES Journal of Marine Science (2012), 69(6), 1099–1107. doi:10.1093/icesjms/fss093

Target strength and tilt-angle distribution of the lesser sandeel (*Ammodytes marinus*)

Rokas Kubilius[1,2]* and Egil Ona[2]

[1]*Klaipeda University, Lithuania*
[2]*Institute of Marine Research, PO Box 1870 Nordnes, NO-5817 Bergen, Norway*

**Corresponding Author: tel: +47 90 36 09 03; fax: +47 55 23 85 32; e-mail: rokas@imr.no*

Kubilius, R., and Ona, E. 2012. Target strength and tilt-angle distribution of lesser sandeel (*Ammodytes marinus*) – ICES Journal of Marine Science, 69: 1099–1107.

Received 26 September 2011; accepted 23 April 2012.

North Sea stocks of lesser sandeel have recently become depleted, and improved methods for abundance estimation are sought. This paper focuses on the acoustic target strength (TS) and orientation of sandeel, measured simultaneously in several field experiments. A specially designed cubic cage, fitted with an echosounder and a video camera, was lowered onto the sea bottom, trapping wild sandeel inside. Methods for manually selecting valid echotraces from individual sandeel are described. Scattered mean TS values from several experiments are reported. These are, in spite of the observed variability, summarized in a TS–fish length (cm) relationship as TS = 20logL – 93.1 (dB) at 200 kHz. We believe that the accuracy of the relationship may still be debated; incorporating larger uncertainty in the overall mean TS will increase the total uncertainty of the stock biomass estimate from sandeel acoustic surveys. This uncertainty is now, using standard narrow-beam echosounders, dominated by the fish patchiness relative to the survey coverage. Results from pilot investigations of the sandeel swimming orientation using video cameras are also presented, showing that sandeel usually has an anguilliform swimming pattern with substantial positive (head-up) tilt. The spread of the tilt-angle distribution is also larger than for more neutrally buoyant fishes.

Keywords: *Ammodytes marinus*, sandeel, target strength, tilt angle.

Introduction

The lesser sandeel (*Ammodytes marinus*) is the most abundant of the five sandeel species found in the North Sea (Macer, 1966). It is an important component in the ecosystem, being available to predators such as fish (Greenstreet *et al.*, 1997; Hislop *et al.*, 1997), mammals (Macleod *et al.*, 2004; Santos *et al.*, 2004), and seabirds. Some of these have already been adversely affected by the depletion of this food source (Furness and Tasker, 2000; Frederiksen *et al.*, 2004; Daunt *et al.*, 2008).

The aggregative and patchy distribution of lesser sandeel (henceforth 'sandeel'; Wright *et al.*, 2000) also makes it an attractive target for commercial fishing. Sandeel became the largest fishery in the North Sea, with landings peaking well above 1 Mt in 1997, with a subsequent stock decline. With decreasing catches, there is a demand for fishery-independent data to support sandeel abundance estimation and management (ICES, 2008).

Earlier acoustic surveys attempted to identify sandeel echotraces by comparing acoustic recordings at two frequencies, 38 and 120 kHz (Hassel *et al.*, 2003; Mackinson *et al.*, 2005). However, description of the technique used was limited, as their investigations had a different focus. Mackinson *et al.* (2005) emphasized lack of certainty about the sandeel target strength (TS), which was critical for their study. The problem of determining the fraction of the population remaining in the sediments (and thus inaccessible to acoustics) while the rest fed in the water column was also stated. More recently, multifrequency acoustics combining 18, 38, 120, and 200 kHz instruments have been successful in identifying and isolating sandeel echotraces among those of mackerel and herring schools (Zahor, 2006). Johnsen *et al.* (2009) showed that the two most abundant sandeel age groups (I and II) can be quite accurately distinguished using multifrequency acoustics. The next challenge was to investigate sandeel TS, which is a key factor in absolute abundance estimation.

The backscattering properties of sandeel have been measured by Armstrong and Edwards (1985) and Armstrong (1986), using a caged ensemble of fish observed over several days at 38 and 120 kHz. They reported a mean TS at 38 kHz of about −72 dB per individual (12–13 cm), or −50 dB/kg. Large, nearly 20 dB (in dB/kg), day–night variations remained unexplained, but were supposed to be caused by changes in the light level, tidal effects, and fish night-time burrowing behaviour. They also

reported 4 dB higher mean sandeel TS at 120 kHz vs. 38 kHz. This is not supported by later multifrequency analyses done by Zahor (2006) and Johnsen *et al.* (2009), which revealed only slight differences in the frequency response of sandeel schools at 38, 120, and 200 kHz. TS modelling at 38 kHz done by Yasuma *et al.* (2009), on the related sandeel species *A. personatus* suggested a mean TS several decibels higher than reported by Armstrong and Edwards (1985, 1986). Further, their modelled maximum TS values were 4–5 dB lower than the near-dorsal aspect measurements of individual *A. hexapterus* reported by Thomas *et al.* (2002).

From an acoustic point of view, sandeel is a challenging object, mainly because it is physically small and a weak acoustic target, but also due to its peculiar behavioural traits. As sandeel forms compact schools in the water column during the day, and subsequently descends into the bottom substrate at dusk, it is almost impossible to resolve this fish as an individual target in the water column using standard split-beam techniques (Ehrenberg, 1983; Sawada *et al.*, 1993; Foote, 1996; Ona, 1999). Therefore, data from *in situ* and *ex situ* TS measurement experiments on enclosed populations of freely swimming sandeel are analysed in this paper. Given the scarce information on sandeel TS currently available, the main objective of this paper is to present new data and findings on this topic.

The mean swimming orientation was also measured from video recordings, as it could help to interpret the observed TS variability. The secondary objective of this work was to provide some first insight on the natural swimming orientation of sandeel for input to acoustic modelling work (Yasuma *et al.*, 2009) and for interpreting the observed variability in the multifrequency response of sandeel schools (Johnsen *et al.*, 2009).

Material and methods

Equipment and experimental design

The acoustic and video camera data were collected during three North Sea sandeel surveys conducted by RV 'Johan Hjort' in April–May 2007, 2008, and 2010. In 2007, a specially designed cage was dropped onto the sea floor at 40 m depth with the bottom side open and left at the bottom for three periods of 4–10 h. The area was a known sandeel ground at 57°10′N 005°33′E. Data from two successful experiments (referred to as experiments A and B) were analysed here. The aim was to trap buried sandeel inside the cage at night; when sandeel ascended from the sediment at dusk and swam inside the cage, the individual TS measurements and video recordings were made. In the 2008 experiment (C), wild sandeel was captured in advance, introduced into the cage, which was later suspended in midwater for acoustic and video measurements. Sandeels were caught by a modified scallop dredge at night when buried in the sediments. The fish were held captive for up to 2 days before experiment C. The storage tank on board the research vessel was cubic with 1.3 m side length, supplied with fresh seawater, and had a 10 cm thick natural sediment layer, earlier obtained from grab samples on the sandeel grounds. After transferring some fish to the cage, it was lowered to ~ 20 m depth in daylight and kept immobile for ~ 3 h. All experiments conducted and data collected are summarized in Table 1.

The cubic metal frame of the cage was made of 30 mm steel pipes, with edge length 2.8 m and covered with 5 mm nylon netting (Figure 1). To trap sandeel fully, 10 cm wide flat iron plates were welded on the bottom frame to ensure proper penetration into the sediments and enclosure of the cage. The control computer and a 200 kHz Simrad EK60 split-beam echosounder were placed in a pressure-resistant aluminium cylinder attached to the metal frame, and connected to an ES-200-7CD transducer located at the centre top of the cage. The batteries powering the system were enclosed in a second pressure-resistant cylinder. After the cage was deployed on the seabed, system performance was checked via a 120 m Ethernet cable. The cable was then disconnected and left in a surface float. The ES-200-7CD transducer had low side lobes (two-way, −52 dB), enabling TS measurements down to −100 dB at short range. The echosounder was calibrated according to standard procedures (Foote *et al.*, 1987; Ona, 1999). Water pressure effects on transducer sensitivity were also considered as described by Ona and Pedersen (2006) and Pedersen *et al.* (2011). The echo sounder settings are listed in Table 2. With no swimbladder, sandeel is generally better detected at higher frequencies, especially smaller individuals (Johnsen *et al.*, 2009). The 200 kHz transducer has a relatively short nearfield range which is relevant for our experimental set-up, but a sufficient effective range for survey purposes.

The cage was also equipped with a high-resolution video camera (Sony HDR-SR1E in 2007, Sony HDR-SR5E in 2008) to ensure successful landing on the seabed, and to obtain some understanding of the sandeel behaviour during the measurements, but not originally with the intention to measure fish-body tilt. The camera was located in the cage corner and observed only the

Table 1. Overview of the experiments conducted.

Experiment	A		B		C	D
Dataset	A1[a]	A2[b]	B1[a]	B2[b]		
Date	25 April 2007		26 April 2007		8 May 2008	20 May 2010
Local time	02:20–12:30		04:40–08:40		18:00–21:00	14:00–15:00
Cage at depth, m	40 (on bottom)		40 (on bottom)		20 (midwater)	On-board tank
Sediment substrate	Yes		Yes		No	Yes
Measurements	*In situ*		*In situ*		*Ex situ*	*Ex situ*
TS	Yes		Yes		Yes	No
Video	No good	Side	No good		Side	Side and dorsal

TS refer to acoustic measurements of sandeel target strength. Video refers to the camera-based sandeel behaviour and swimming pattern measurements from side and dorsal aspects. Availability of sediment substrate for sandeel to hide in or rest is also indicated.
[a]Observations during first 10 min after cage landing on the sea bottom, see text.
[b]Observations obtained after first 10 min during the main experiment, see text.

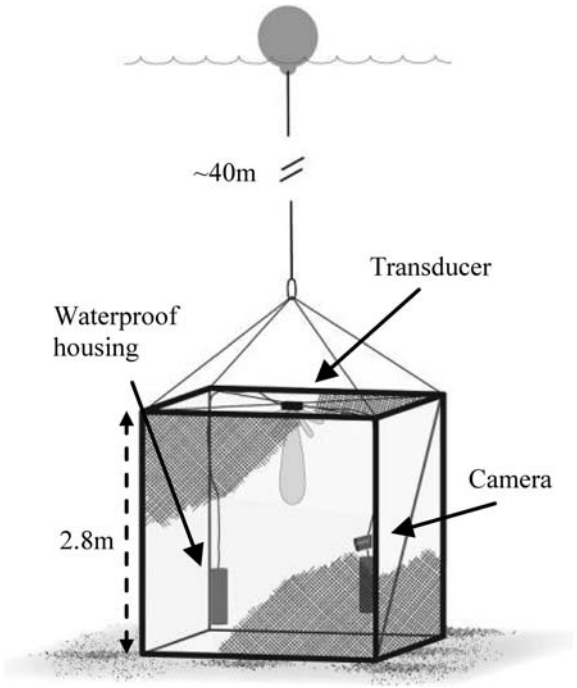

Figure 1. Schematic view of the sandeel cage. The transducer is mounted at the centre top of the cage, connected to two underwater housings for instruments and battery. The video camera is on the right-hand side of the cage.

Table 2. Calibration data and parameter settings of the echo sounder mounted on the sandeel cage in both 2007 (experiment A and B) and 2008 (experiment C).

Parameter	2007 and 2008
Transducer type	ES-200-7CD
Transmission frequency (kHz)	200
Transmission power (W)	300
Bandwidth (kHz)	15.73
Pulse duration (ms)	0.128
Ping interval (s)	0.1
Transducer angle sensitivity (along ship and athwart ship)	23.0
Equivalent beam angle (dB)	−20.7
Digital sample distance (cm)	2.4
TS transducer gain (dB)	−26.8
Half power beam widths (°)	6.95/6.94 (7.00/7.00)
Absorption coefficient (dB km^{-1})	47.3
Sound speed (measured; m s^{-1})	1488

The parameter in parentheses was obtained in 2008 and was the only one that differed between the years.

central part of the cage; it was fixed tilting downwards in experiments A and B, but could be rotated up and down by a motor in experiment C. No artificial light was used.

Observations of the general swimming pattern were also made on fish in the storage tank (cubic, 1.3 m side length) onboard the research vessel. About 150 sandeels caught by modified dredge in the 2010 sandeel survey were transferred into the tank and kept there during the survey. The fish behaviour and swimming orientation were recorded by a video camera (Sony HDR-SR5E) first from the side, then from the dorsal aspect for 1 h in total (referred to as experiment D). A nylon plumb line was placed in front of the camera as a vertical reference when recording videos from the side aspect. The aim was to record the body shape during swimming, for later model calculations of the sandeel backscattering properties and to support or falsify the swimming behaviour recorded in the cage.

Acoustic data analysis

The range window for accepting single-fish targets was 1.1–2.7 m in front of the transducer; 1.1 m corresponds to about double the acoustic nearfield distance for the 200 kHz transducer used. This wide range was necessary due to the extensive vertical distribution of targets and the limited number of single-fish detections. Filtering of small free-drifting zooplankton was done by careful manual selection of single-fish tracks using the LSSS acoustical post-processing software (Korneliussen *et al.*, 2006). Visual identification of fish traces on the echogram was usually based on track speed; track length was much longer for the slowly drifting plankton than for the fish (Figure 2). The TS measurements of individual sandeel were done by the single-echo detection (SED) method (Handegard *et al.*, 2005; Handegard, 2007), averaged in the linear domain. The SED settings are listed in Table 3; for a detailed description of detector filters and the single acoustic target detection principle, see Ona (1999).

The information collected about each TS detection included: the time, range from transducer, beam-compensated TS, beam-uncompensated TS, and the target in-beam position angles α (athwart ship) and β (along ship). The main challenge was the weak backscattering of single sandeel targets (−85 to −55 dB), which partly overlapped with echoes from drifting zooplankton (−90 to −75 dB). The mean TS estimates by fish length were further summarized by calculating the so-called reduced target strength b20, from the formula $TS = 20\log L + b20$, as the fitted mean TS–length relationship (Simmonds and Maclennan, 2005). The slope in this relationship is supported by TS modelling on adult *A. personatus*, a close relative to our species (Yasuma *et al.*, 2009).

Video data analysis

After three successful sandeel cage experiments, ~ 11 h of video data were available. These were not originally collected for tilt-angle measurements. However, it was later realized that the records contained substantial information which could be used for interpreting the acoustic data. Since the camera was tilted out of the horizontal plane, it was a challenge to extract fish-body tilt angles in the vertical plane from pictures taken in another plane. A method for obtaining the fish tilt angle from such data is described by Kubilius (2009), who concluded that the measurement accuracy was about ± 2–3°, when fish are passing with $<10^\circ$ angle off the plane perpendicular to the camera focal axis. This is less compared with the fish-body tilt measurement accuracy of about $\pm 1^\circ$ obtained with a horizontally mounted camera. However, the general shape and statistical parameters of the tilt-angle distribution can be described quite accurately if the distribution is relatively wide.

The 2010 video data (experiment D) were collected with the camera's optical axis being horizontal, and these were analysed in the classical way for one-camera datasets (see, for example, Olsen, 1971; Carscadden and Miller, 1980; Foote and Ona, 1987), using a plumb line in front of the lens as a vertical reference.

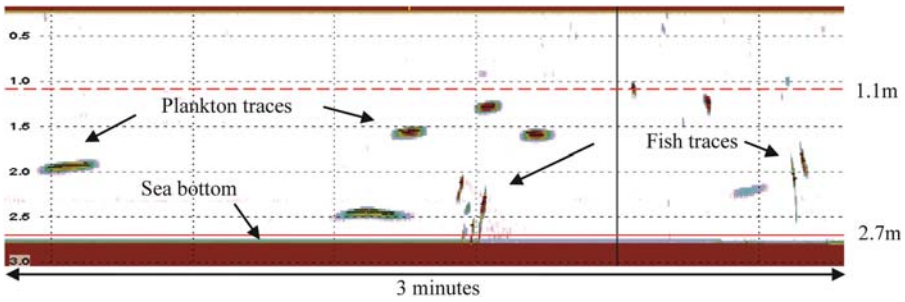

Figure 2. Example echogram (experiment A), showing the distinction between sandeel and zooplankton traces. Vertical scale 3.0 m; ping repetition frequency 10 s^{-1}.

Table 3. Single echo detector settings used in the target strength analysis.

Parameter	Settings
Minimum TS (dB)	−95
Min/max echo length (relative to pulse length)	0.8, 1.8
Maximum phase deviation (°)	7.0
Maximum gain compensation (dB)	6
Minimum echo spacing (samples)	1
Cut-off angle (∼half power angle) (°)	3.5

Cut-off angle is the maximum angle from the acoustic axis for accepted targets.

Selected still frames were used to measure the body tilt of fish considered to be $<10^{\circ}$ out of the photo plane. The estimated tilt measurement accuracy here was $\pm 1{-}2^{\circ}$. This was mostly due to slight vessel movement, as evident from the plumb line that was measured at every frame. Dorsal aspect sandeel imagery was also collected in experiment D. These were used to measure the sandeel body movements during swimming.

Pictures from video data were extracted and enhanced using a special video editing software (Video to JPG Converter, 2009). In experiments A and C, single frames at a rate of 15 frames s^{-1} were extracted from the video data. The same fish could then be measured several times over a single passage in front of the camera. As many more (∼50–60) sandeels per frame were recorded on the video from the on-board fish tank (experiment D), an extraction rate of 1 frame per 5 s was used here. This better ensured random, uncorrelated fish orientations in each frame. Further enhancement and analysis on each frame was done using photo editing software ImageJ, version 1.43u (ImageJ, 2009). Example pictures are shown in Figure 3.

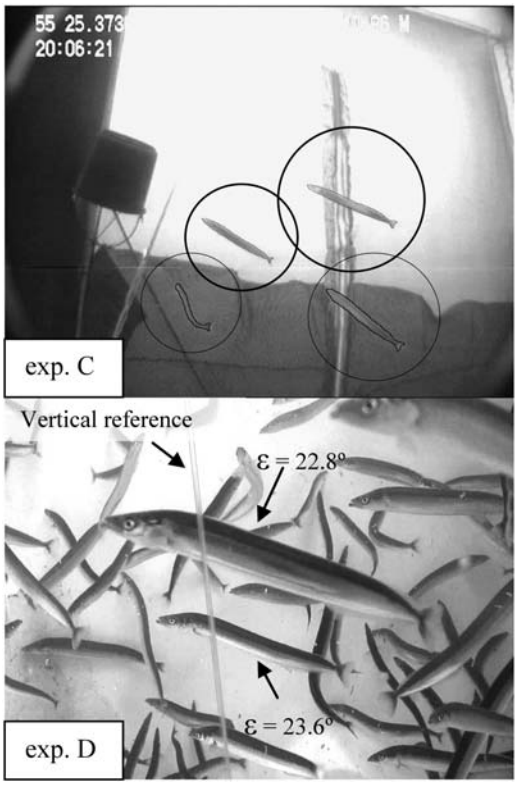

Figure 3. Common sandeel swimming orientation, as observed in experiments C and D. In experiment C, sandeels are in a free-hanging cage at 20 m depth. In experiment D, sandeels are in an on-board fish tank. ε is body tilt from the horizontal.

Sandeel nearfield

The fish as an acoustic target has its own nearfield, which must be considered when measurements are made at short range. This depends on the whole-body length projection in the plane perpendicular to the acoustic axis of the transducer when (as with sandeel) there is no dominating reflector such as a swimbladder inside the target. The sandeel examined in this work normally swam with anguilliform locomotion and substantial tilt. Both of these effects reduce the target nearfield distance, as compared with one of a fully stretched and horizontal fish.

The effective shortening of sandeel body length by anguilliform swimming was estimated from video data on the dorsal aspect of sandeel in a tank (experiment D). The length of fish swimming in the horizontal plane was calculated in relative units, i.e. the number of pixels between 30 and 50 points placed along the sandeel body length. Sandeel body linear length was defined as a line between the two most distant points which are the root of the tail and the tip of the snoot. The sandeel nearfield was calculated using the expression $D = r^2/\lambda$, where r is fish half-length and λ is length of the sound wave (Medwin and Clay, 1998).

Results

Sandeel target strength

Five mean TS estimates from three independent experiments (A, B, and C) were obtained. The TS distributions of the manually selected targets are shown in Figure 4a–e. The acoustic data

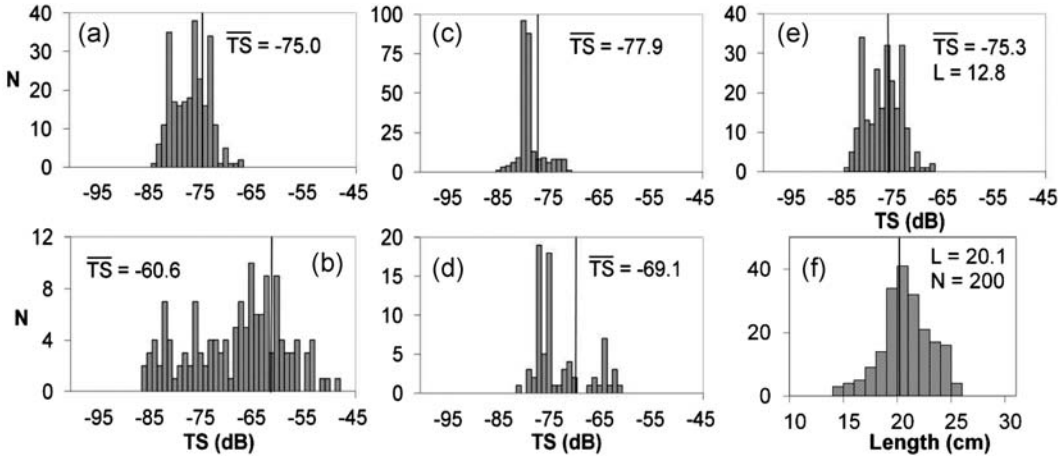

Figure 4. Sandeel target strength (TS) distributions with their mean values also shown on the histograms as vertical dark lines. (a) Experiment A, first 10 min after cage landing (A1), (b) experiment A, main experiment (A2), (c) experiment B, first 10 min after cage landing (B1), and (d) experiment B, main experiment (B2). (e) Sandeel TS measurements from experiment C. (f) Sandeel length distribution from trawl catches close to the deployment sites of experiments A and B. N is count/sample size, L is mean fish length in cm.

from experiments A and B were both divided into two datasets. Acoustic data within ~10 min just after cage landing were qualitatively different from the data recorded later on. They contained many more targets in the water column, including many TS detections from disturbed and actively swimming sandeel (Figure 4a and c). It was more challenging to identify sandeel in this part of the data, as most of them were not well resolved into single tracks, and acceptance of a few missinterpreted plankton targets was therefore likely. The sandeel disturbed just after landing of the cage were also expected to have different swimming behaviour compared with later, when it had calmed down. Therefore, these data were treated separately as datasets A1 and B1, but are not dismissed as the data and knowledge on sandeel TS are scarce. The data from the main experiment are datasets A2 and B2 (Figure 4; also see Table 1).

TS estimates for the main part of experiments A (A2, Figure 4b) and B (B2, Figure 4d) were considered to be particularly good quality, because sandeel tracks were easy to identify and isolate from other targets (Figure 2). The bimodal TS distribution seen in Figure 4d may have occured due to small sample size ($n = 75$).

The sandeel cage experiment in 2008 (experiment C) was performed using fish captured in advance, and a totally enclosed cage. Since the cage was suspended in midwater, the transducer and cage moved slightly with sea-wave motion, making target tracking more difficult than in the stationary cage. Nevertheless, C is considered to be a good-quality dataset as sandeel had distinctively shorter track lengths than free-drifting particles; TS results are presented in Figure 4e.

There was a wide spread of TS values within each dataset, typically 20 dB. The largest TS variability and the highest mean value were found in the A2 data (Figure 4b). The records at the lower end of the TS distributions may to some extent be zooplankton targets. This may also have contributed to the high peaks in the TS distribution for the datasets obtained just after cage landing (A1 and B1, Figure 4a and c), where sandeel target recognition was more challenging. Finally, all five mean TS estimates were combined to yield the regression: TS = 20logL − 96.9 dB, as the TS–length relationship for sandeel. If the analysis were restricted to the most trusted TS datasets (A2, B2, and C) with least disturbed sandeel behaviour, then the regression would be: TS = 20logL − 93.1 dB. Since the length variation was very limited, no attempt was made to estimate the slope of the regression.

In 2007 (A and B), the cage had no closing device and the fish size distribution had to be determined indirectly, from samples caught by trawling and dredging in the vicinity of the experimental site. The mean length of the sampled sandeel was 20.1 cm with 95% confidence interval (CI) ±0.3 cm (Figure 4f); this was assumed to be representative for sandeel observed inside the cage. The fish used in experiment C were captured in advance; their average length was 12.8 cm with 95% CI ±0.8 cm.

The video recordings showed no fish other than sandeel within the cage. However, since only a small fraction of the cage volume was observed by camera, other species of fish could have been present in A and B. Some non-sandeel traces, most probably due to a small flatfish, were identified acoustically in the B2 data, as strong TS records close to the seabed. These records were removed from the sandeel dataset.

The average compensated and uncompensated for beam pattern TS (TSC and TSU) are presented in Table 4, where b20 is also listed. The TSU was lower than TSC by an average of 2.5 dB. The TS detections were found to be randomly distributed across the acoustic beam in the A1, A2, and C datasets (χ^2 goodness of fit test, $p > 0.05$). Because of the narrow beam, short range, and relatively high sandeel swimming speed, only a few TS detections were obtained on each passing fish. If the detected targets passed randomly across the beam, a fixed correction for the beam-pattern loss may be applied to TSU. Data recorded using calibration spheres were used to estimate the mean beam correction factor, presented in Table 4. The TS measurements, compensated for the beam-pattern loss in two different ways, can be now compared (TSA vs. TSC in Table 4).

Sandeel orientation

The video records from experiments A, C, and D were examined to identify fish with the body axis in or near the plane perpendicular to the camera's focal axis. The analysis of all A and C video data

Table 4. The mean beam compensated target strength (TSC) and the mean beam uncompensated target strength (TSU) are shown for each experiment along with TSA [target strength adjusted by a fixed, average acoustic beam compensation factor (mean 2B, α, β), measured on a calibration sphere with 3.5° cut-off angle]. An unweighted mean b20 is also given. L refers to the mean fish length.

Dataset	L (cm)	TSC (dB)	TSU (dB)	Mean 2B (α, β) (dB)	TSA (dB)
A1	20.1	−75.0	−77.5	3.2	−74.3
A2	20.1	−60.6	−62.8	3.2	−59.6
B1	20.1	−77.9	−80.4	3.2	−77.2
B2	20.1	−69.1	−71.8	3.2	−68.6
C	12.8	−75.3	−77.9	3.2	−74.7
b20		−96.9	−99.4		−96.2

resulted in total of 507 sandeel body tilt measurements with about equal contribution from both datasets. These were considered to be most valuable as measured *in situ* (A) and in the more natural environment of a suspended sandeel cage (C), if compared with a small on-board fish tank (D). Therefore, 534 fish tilt measurements from the D dataset were thought to be sufficient to support or falsify the results from experiments A and C.

The following results show the mean tilt angle (ε) per experiment, with a range representing the 95% CI for the mean, and the sample standard deviation (SD). For experiment A, ε was not significantly different from zero ($1.8 \pm 3.1^\circ$ SD $= 24.1^\circ$; $n =$ 236; Figure 5a). However, few tilt values were found close to the mean value. If the tilt sign is ignored, the results give a mean tilt of 20.4° ($\pm 1.7^\circ$; SD $= 13.1^\circ$). The latter value is probably more relevant to the acoustic measurements, especially as the sandeel has no dominant scattering organ such as a swimbladder. Due to the poor visibility in the morning twilight, only the later part of experiment A video data yielded tilt measurements; these are therefore relevant for interpreting the A2 acoustic dataset. The C video data were of good quality throughout the acoustic data collection period. In this case the video analysis revealed significant positive tilt angles ($\varepsilon = 23.3 \pm 3.0^\circ$; SD $= 25.4^\circ$; $n = 271$; Figure 5b). The experiment D analysis yielded similar results ($\varepsilon = 23.7 \pm 1.5^\circ$; SD $= 18.2^\circ$; $n = 534$; Figure 5c). The commonly observed sandeel swimming behaviour is illustrated by the photos in Figure 3. No useful body tilt data could be extracted from B due to the poor video quality.

Some behavioural differences were observed between the experiments: A revealed more or less random sandeel swimming directions while in C the fish tended to swim in groups with similar, mostly positive tilts, as is typical for schools (Figure 3). In both experiments, the video camera observed only the central part of the cage. Sandeels remained in the camera observation volume for several seconds. However, a fraction of the fish could suddenly change their swimming direction while still in the camera view, sometimes more than once in A. Most of the sandeels were observed to swim at low speed with body tilts very different from those estimated from acoustic target tracking in C and A. This suggests that sandeels were negatively buoyant and that a positive lift is generated at slow swimming speed by moving with a head-up posture. Sandeel body tilt angle is different from the swimming track angle. The target tracking method for determining fish tilt angle, as suggested possible for herring by Ona (2001), is therefore invalid for sandeel.

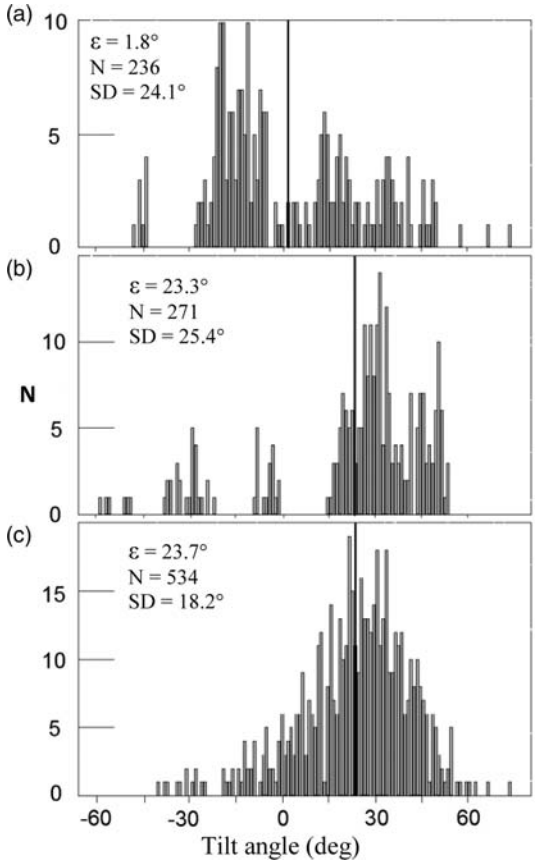

Figure 5. Sandeel tilt-angle distributions obtained from: (a) experiment A, (b) experiment C, and (c) experiment D video datasets. ε is mean tilt angle (positive is head-up), also shown by the vertical dark lines on the histograms. N is sample size, SD is the standard deviation.

Consideration on nearfield range

The sandeel nearfield extent was found to be substantially reduced by eel-like swimming behaviour and tilt. The average reduction in fish nearfield range by the combined effect of S-shaped swim and tilt can be expressed as: $1 - [k \cos(\phi)]^2$, where ϕ is the tilt angle and k is the linear sandeel body length compression factor due to the anguilliform swimming pattern. The tail of the sandeel is a very weak scatterer, and the root of the fish tail should preferably be used when estimating the effective nearfield.

Ignoring the tail shortens the sandeel body length by 5.3% (average for ten fish measured on free-swimming fish in experiment D). The linear body length compression due to S-shape swimming was on average $6.7 \pm 1.0\%$ as 95% CI (SD $= 5.0\%$; $n = 100$; experiment D). For 12.8 cm fish with 23.3° tilt and 6.7% shorter linear body length, the estimated nearfield was shorter by 26.6% or 0.36 m as the total extent (C situation). For sandeel of 20.1 cm length with 20° tilt and 6.7% effective body length shortening by swimming in an S-shape, it was shorter by 23.1% or 0.94 m as the full extent nearfield range (A and B situation). Following this, the chosen minimum range for accepted acoustic targets was 1.10 m; this accounts for more than twice the transducer nearfield distance, more than once the fish nearfield distance in A and B, and more than three times the fish nearfield distance in C. MatLab simulations, calculating the nearfield from a

15 cm chain of 6 mm radius elastic spheres (Professor Halvor Hobaek, pers. comm. 2010), also indicate that for tilt angles outside broadside incidence, the far field starts at <1.0 m at 200 kHz.

Discussion

Sandeel TS

The amount of TS data collected was rather limited. The first of the 2007 experiments failed; the other two (A and B) were successful, but still only few fish were trapped inside the cage. The experiment in 2008 (C), with fish caught in advance and introduced into the cage, yielded a more comprehensive dataset. However, other problems limited the C data. The sandeel tended to swim closer to the transducer here, inside the nearfield where no useful measurements could be made.

It is important to note that the targets were recorded at distances <3 m in front of the transducer. The eel-like and tilted swimming behaviour of the sandeel effectively reduced the nearfield range of the fish itself. Considering the nearfields of both the transducer and the target, we believe the acoustic measurements at the distances in question (1.1–2.7 m) are valid.

The sandeel length, if horizontal and fully stretched, was close to the diameter of the acoustic beam in these experiments. The accuracy of split-beam positioning and beam compensation may then be questioned, even though it seems to work well from track to track observations. Having in mind random across-beam distribution of TS detections for most of the datasets and stable TSC and TSU difference between datasets, the compensation for beam pattern is thought to be more or less valid. The average TSU, which includes no compensation for the acoustic beam pattern, was also calculated (Table 4) and compensated with a mean beam correction factor. The latter is presented in order to demonstrate relatively small differences between the compensation for acoustic beam pattern as measured in our sandeel TS data and when measured on a calibration sphere placed well in the far field of the transducer (TSC vs. TSA in Table 4).

The sandeel is normally a schooling fish; therefore, on acoustic abundance estimation surveys, schools are usually identified and measured, rather than individual fish. The mean TS of individual sandeel in the cage could differ from that of wild fish in natural schools, due to behavioural differences especially in their body orientation pattern. Intrinsic knowledge on the backscattering is however obtained, and the present experiments are just one of the steps needed to understand fully the sandeel TS.

The presence of non-sandeel fish inside the cage was a possible error source, since the investigated fish could not be caught and physically examined in experiments A and B. This should lead to minor bias, however, because the video records showed only sandeel and the occasional flatfish outside the cage. The nearby trawl catches also indicated a very large (190:1) ratio of sandeel to flatfish by numbers.

Considerable differences in the sandeel average TS estimates were observed between datasets (Figure 4). The A1 and B1 datasets were obtained on the possibly disturbed sandeel just after the cage had landed. It is therefore likely that the low TS values recorded in A1 and B1 were caused by unusually high body tilts associated with escape behaviour of the fish. A fraction of the high peaks in Figure 4a and c might also be due to misinterpreted plankton targets.

Experimental conditions were similar for the A2 and B2 datasets. It remains unclear why the TS estimates from these two datasets are very different. The mean sandeel tilt angle, measured at a period corresponding to the A2 dataset, was close to horizontal, which might partly explain the higher average TS estimate (Figures 4b and 5a). On the other hand, few of the tilt measurements were close to the mean; most had large positive or negative values. Since the cage had no closing device, trapping different sizes of sandeel inside the cage could also be a possible explanation for the TS variation. However, the sandeel size distribution from trawl catches close to the sites of experiment A and B was unusually narrow and unimodal (Figure 4f).

Smaller sandeel were observed in experiment C (average length 12.8 cm) than in A and B (average length 20.1 cm). Lower TS estimates were therefore expected. Furthermore, the mean tilt angle was large and positive 23.3°, suggesting that the fish-body orientation may be important in explaining the different TS results in C compared with A2.

Most of the results presented in this paper show lower sandeel TS than those reported by Armstrong and Edwards (1985) and Armstrong (1986). There were large variability and cyclic changes in their TS data, with widely scattered mean TS estimates from successive experiments. Strong diel cycles in the measured TS could be explained by the possible influence of changing light levels, the burrowing behaviour of sandeel, and/or tidal effects. The last two might well have contributed error in the highest TS measurements, due to the fish adopting unnatural, near-horizontal body tilts. Only slight differences in the frequency response of sandeel schools have been demonstrated at 38 and 200 kHz by Zahor (2006) and Johnsen *et al.* (2009), at least for the most common age groups, 1 and 2 year olds. The mean difference in frequency response of sandeel schools detected at 38 and 200 kHz was shown to be <1.0 dB (for details see Johnsen *et al.*, 2009). The b20, based on all TS datasets collected here, was lower than that of Armstrong and Edwards (1985) and Armstrong (1986) by 2 dB. However, this difference is small considering wide scatter of average TS from our and their datasets (Figure 6). If only the most trusted TS datasets are considered (undisturbed sandeel in A2, B2, and C), the calculated b20 would be higher than in Armstrong and Edwards (1985) and Armstrong (1986). The modelling results of Yasuma *et al.* (2009) were somewhat higher (b20 was −89.2 dB at 38 kHz and −92.1 dB at 120 kHz) than most of the empirical results shown in Figure 6. However, their modelling assumed a tilt-angle distribution with a mean of 0° and SD of 15°. Our observations on freely swimming sandeel show that the average body tilt is generally high and positive (head-up). The results from various sources compared in Figure 6 clearly illustrate the very large uncertainty about the mean TS of sandeel.

In conclusion it can be said that at present, no useful 'true' mean TS can be stated for sandeel, and further investigation is still needed. The observed variability in both the current and earlier measurements indicates that behavioural effects on TS are much larger for sandeel than for other, more neutrally buoyant fish species.

Sandeel orientation

It is well known that an important factor influencing the mean acoustic backscattering from a fish is the body orientation relative to the acoustic wave front (Nakken and Olsen, 1977; Foote, 1980). For conventional downward-looking echosounders, the fish-body tilt in the vertical plane is the key factor, as acoustic directivity changes little with roll angle (Haslett, 1977; Nakken and Olsen, 1977). The sandeel is large enough to be a directive scatterer at

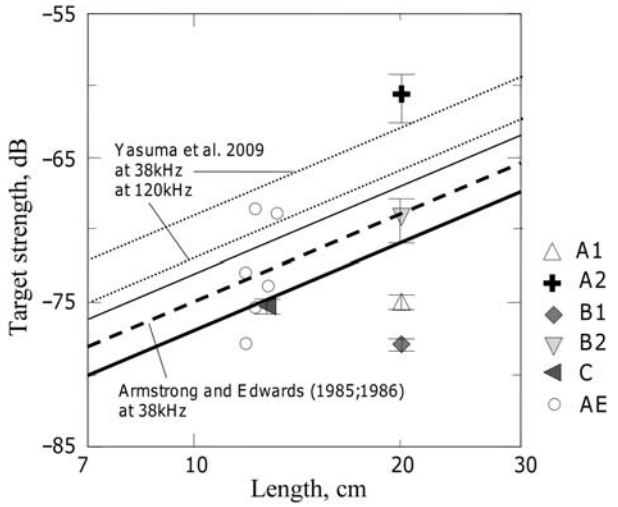

Figure 6. Sandeel mean TS measurements plotted against fish length in logarithmic scale. Points are mean values per dataset (with horizontal bars showing the 95% confidence intervals); lines are TS = 20logL + b20 least-squares regressions; AE and the dashed line are Armstrong and Edwards (1985) and Armstrong (1986) data at 38 kHz; A1, A2, B1, B2, and C, and the solid thick line (regression using all these data) are results from the present experiments; the solid thin line is the regression using the (A2, B2, C) data only; the dotted lines Y38 and Y120 are modelling results on *A. personatus* from Yasuma *et al.* (2009) for 38 and 120 kHz, respectively.

the 200 kHz frequency used here. Information on the swimming behaviour, especially the tilt angle of this fish, may help to explain the large variation in the measured TS. An unconventional method had to be used (Kubilius, 2009) to estimate the tilt angle from video data recorded with the camera tilted away from the horizontal, but was shown to give results good enough to elucidate some of the observed TS variation.

Probably the most important error source was in selecting images of sandeel that were within $\pm 10^\circ$ off the plane perpendicular to the camera's focal axis. The analysis assumes that the fish are in the focal plane, and any off-plane angle introduces an error in the tilt-angle estimate. However, if only fish within $10-20^\circ$ off-plane were considered, the error was acceptable, at least for these first attempts to investigate sandeel orientation (Kubilius, 2009). The estimated accuracy of the tilt-angle measurements was $\pm 2-3^\circ$ in A and C, and $\pm 1-2^\circ$ in D imagery analysis. This is good enough to provide useful data when the tilt-angle variability is high, as here.

Large variability in measured sandeel tilts was observed (Figure 5), as well as a substantial difference between sandeel mean tilt-angle estimates. Differing experimental designs and environments for sandeel could deliver possible explanations for such a disparity. In experiment A the cage was on the sea floor at a depth of ~40 m, where there was less light, and no cage movement and bottom sediment available for the sandeel to hide in.

During experiments C and D, there was more ambient light around the fish and slight cage movement due to sea waves. The multimodal nature of the distributions in Figure 5 is thought to be caused by the relatively small sample size, as behaviour of distinct single animals could still be recognized in the histograms. According to Henderson *et al.* (2007), the effect of fish-body tilt on the mean TS is greatly reduced when the standard deviation of the tilt angle measurements is $>20^\circ$.

The sandeel tilt angle cannot be measured using split-beam acoustic target-tracking techniques. These measure the tilt of the swim track, but we observed sandeel swimming slowly with body-tilt angles much greater than the angle of the swim track. The fish-body and swim-track angles of this fish (see Ona, 2001) can be very different, often by as much as 20° due to hydrodynamic compensation for negative buoyancy.

The body tilt of the lesser sandeel or any closely related species has, to our knowledge, not previously been examined experimentally. However, it seems that many fish with swimbladders have close to horizontal mean tilt angles: cod (-4.4°, SD = 16.2°; Olsen, 1971), capelin (3.8°, SD = 18.4°; Carscadden and Miller, 1980), caged saithe (-0.9°, SD = 5.4°; Foote and Ona, 1987), and hoki (11.8°, SD = 29.9°; Coombs and Cordue, 1995). Those with no swimbladder, such as mackerel or sandeel, are generally negatively buoyant, and they must swim with some positive body tilt to maintain altitude. Sandeel is a schooling plankton feeder that strongly associates with the preferred sea bottom substrate (Macer, 1966; Wright *et al.*, 2000); schools of sandeel seen on echograms often have contact with the seabed, and they can repeatedly be observed in the same position, which suggests that sandeel tend to stay and forage within a small area. Thus the sandeel has no need to swim fast. Its average body-tilt angle is likely to be large and positive. Our results from experiment C and D showing average body tilts of 23.3° and 23.7° might be a good approximation to the natural behaviour of this species in a foraging situation, notwithstanding the limited data available. The results in this paper should be considered as a pilot investigation of sandeel swimming behaviour and natural body tilts. However, we have shown that fish-body orientations measured simultaneously with the target strength can be very helpful when interpreting acoustic data.

Acknowledgements

Senior engineers Ingvald Svellingen, Roar Skeide, and Ronald Pedersen are thanked for their skilful equipment design and operation of the experimental cage. Also the crew of RV Johan Hjort is thanked for their cooperation during the work. The Research Council of Norway is thanked for its financial contribution to the sandeel project under contract 185065/S40.

References

Armstrong, E. 1986. Target strength of sandeels. ICES Document CM 1986/B: 5. 5 pp.

Armstrong, E., and Edwards, J. I. 1985. Target strength of sandeels. ICES Document CM 1985/B: 20. 5 pp.

Carscadden, J. E., and Miller, D. S. 1980. Estimates of tilt angle of capelin using underwater photographs. ICES Document CM 1980/H: 50. 4 pp.

Coombs, R. F., and Cordue, P. L. 1995. Evolution of a stock assessment tool: acoustic surveys of spawning hoki (*Macruronus novaezelandiae*) off the west coast of the South Island, New Zealand, 1985–1991. New Zealand Journal of Marine and Freshwater Research, 29: 175–194.

Daunt, F., Wanless, S., Greenstreet, S. P. R., Jensen, H., Hamer, K. C., and Harris, M. P. 2008. The impact of the sandeel fishery closure on seabird food consumption, distribution, and productivity in the northwestern North Sea. Canadian Journal of Fisheries and Aquatic Sciences, 65: 362–381.

Ehrenberg, J. E. 1983. New methods for indirectly measuring the mean acoustic bacscattering cross-section of fish. FAO Fisheries Report, 300: 91–98.

Foote, K. G. 1980. Effect of fish behaviour on echo energy: the need for measurements of orientation distributions. Journal du Conseil International pour l'Exploration de la Mer, 39: 193–201.

Foote, K. G. 1996. Coincidence echo statistics. Journal of the Acoustical Society of America, 99: 266–271.

Foote, K. G., Knudsen, H. P., Vestnes, G., MacLenan, D. N., and Simmonds, E. J. 1987. Calibration of acoustic instruments for fish density estimation: a practical guide. ICES Cooperative Research Report, 144: 69 pp.

Foote, K. G., and Ona, E. 1987. Tilt angles of schooling penned saithe. Journal du Conseil International pour l'Exploration de la Mer, 43: 118–121.

Frederiksen, M., Wanless, S., Harris, M. P., Rothery, P., and Wilson, L. J. 2004. The role of industrial fisheries and oceanographic change in the decline of North Sea black-legged kittiwakes. Journal of Applied Ecology, 41: 1129–1139.

Furness, R. W., and Tasker, M. L. 2000. Seabird–fishery interactions: quantifying the sensitivity of seabirds to reduction in sandeel abundance, and identification of key areas for sensitive seabirds in the North Sea. Marine Ecology Progress Series, 202: 253–264.

Greenstreet, S. P. R., Bryant, A. D., Broekhuizen, N., Hall, S. J., and Heath, M. R. 1997. Seasonal variation in the consumption of food by fish in the North Sea and implications for food web dynamics. ICES Journal of Marine Science, 54: 243–266.

Handegard, N. O. 2007. Observing individual fish behaviour in fish aggregations: tracking in dense fish aggregations using a split-beam echosounder. Journal of the Acoustical Society of America, 122: 177–187.

Handegard, N. O., Patel, R., and Hjellvik, V. 2005. Tracking individual fish from a moving platform using a split-beam transducer. Journal of the Acoustical Society of America, 118: 2210–2223.

Haslett, R. W. G. 1977. Automatic plotting of polar diagrams of target strength of fish in roll, pitch and yaw. Rapports et Procès-Verbaux des Réunions du Conseil International pour l'Exploration de la Mer, 170: 74–81.

Hassel, A., Knutsen, T., Dalen, J., Skaar, K., Østensen, Ø., Haugland, E. K., Fonn, M., *et al.* 2003. Reaction of sandeel to seismic shooting: A field experiment and fishery statistics study. Fisken og Havet, Institute of Marine Research, Norway, 4: 62 pp.

Henderson, M. J., Horne, J. K., and Towler, R. H. 2007. The influence of beam position and swimming direction on fish target strength. ICES Journal of Marine Science, 65: 226–237.

Hislop, J., Bromley, P. J., Daan, N., Gislason, H., Heessen, H. J. L., Robb, A. P., Skagen, D., *et al.* 1997. Database Report of the Stomach Sampling Project, 1991. ICES Cooperative Research Report, 219: 1–422.

ICES. 2008. Report of the ICES Advisory Committee, 2008. Book 6. North Sea. 50–53.

ImageJ. 2009. Open source software, developed by W. S. Rasband, Research Services Branch, National Institute of Mental Health, Bethesda, Maryland, USA. Available at: http://rsb.info.nih.gov/ij/.

Johnsen, E., Pedersen, R., and Ona, E. 2009. Size-dependent frequency response of sandeel schools. ICES Journal of Marine Science, 66: 1100–1105.

Korneliussen, R. J., Ona, E., Eliassen, I., Heggelund, Y., Patel, R., Godø, O. R., Giertsen, C., *et al.* 2006. The Large Scale Survey System—LSSS. Proceedings of the 29th Scandinavian Symposium on Physical Acoustics, Ustaoset, Norway, January 29–February 1, 2006.

Kubilius, R. 2009. Target strength and tilt angle distribution of lesser sandeel (*Ammodytes marinus*). Masters thesis, Klaipeda University, 64 pp. Available online: http://brage.bibsys.no/imr/handle/URN:NBN:no-bibsys_brage_18624.

Macer, C. T. 1966. Sandeels (Ammodytidae) in the south-western North Sea: their biology and fishery. Fishery Investigations, Ministry of Agriculture, Fisheries and Food, Series II, 24. 55 pp.

Mackinson, S., Turner, K., Righton, D., and Metcalfe, J. D. 2005. Using acoustics to investigate changes in efficiency of a sandeel dredge. Fisheries Research, 71: 357–363.

Macleod, K., Fairbairns, R., Gill, A., Fairbairns, B., Gordon, J., Blair-Myers, C., and Parsons, E. C. M. 2004. Seasonal distribution of minke whales Balaenoptera acutorostrata in relation to physio-graphy and prey off the Isle of Mull, Scotland. Marine Ecology Progress Series, 277: 263–274.

Medwin, H., and Clay, C. S. 1998. Fundamentals of Acoustical Oceanography. Academic Press Limited, London, 142–143.

Nakken, O., and Olsen, K. 1977. Target strength measurements of fish. Rapports et Procès-Verbaux des Réunions du Conseil International pour l'Exploration de la Mer, 170: 52–69.

Olsen, K. 1971. Orientation measurements of cod in Lofoten obtained from underwater photographs and their relation to target strength. ICES Document CM 1971/B: 17. 8 pp.

Ona, E. (Ed.) 1999. Methodology for target-strength measurements (with special reference to *in situ* techniques for fish and micronekton). ICES Cooperative Research Report 235, Prepared by the Study Group on Target Strength Methodology. 58 pp.

Ona, E. 2001. Herring tilt angles, measured through target tracking. Lowell Wakefield Fisheries Symposium Series no. 18. Herring. Expectations for a New Millennium, 509–519.

Ona, E., and Pedersen, G. 2006. Calibrating split beam transducers at depth. Journal of the Acoustical Society of America, 120: 3017.

Pedersen, G., Godø, O. R., Ona, E., and Macaulay, G. 2011. A revised target strength–length estimate for blue whiting (*Micromesistius poutassou*): implications for biomass estimates. ICES Journal of Marine Science, 68: 2222–2228.

Santos, M. B., Pierce, G. J., Learmonth, J. A., Reid, R. J., Ross, H. M., Patterson, I. A. P., Reid, D. G., *et al.* 2004. Variability in the diet of harbor porpoise (*Phocoena phocoena*) in Scottish waters 1992–2003. Marine Mammal Science, 20: 1–27.

Sawada, K., Furusawa, M., and Williamson, N. I. 1993. Conditions for precise measurements of fish target strength in situ. Journal of the Marine Acoustical Society of Japan, 20: 15–79.

Simmonds, J., and Maclennan, D. 2005. Fisheries Acoustics. Theory and Practice, 2nd edn. Blackwell Publishing, Oxford. 437 pp.

Thomas, G. L., Kirsch, J., and Thorne, R. E. 2002. Ex situ target strength measurements of Pacific herring and Pacific sand lance. North American Journal of Fisheries Management, 22: 1136–1145.

Video to JPG Converter. 2009. Software Free Video to JPG Converter 1.7.4.61 is available at: http://www.dvdvideosoft.com/products/dvd/Free-Video-to-JPG-Converter.htm.

Wright, P. J., Jensen, H., and Tuck, I. 2000. The influence of sediment type on the distribution of the lesser sandeel, Ammodytes marinus. Journal of Sea Research, 44: 243–256.

Yasuma, H., Nakagawa, R., Yamakawa, T., Miyashita, K., and Aoki, I. 2009. Density and sound-speed contrasts, and target strength of Japanese sandeel Ammodytes personatus. Fisheries Science, 75: 545–552.

Zahor, M. 2006. Acoustic identification of sandeel (*Ammodytes marinus*) using multi-frequency methods. Masters Thesis, University of Bergen, 68 pp.

Handling editor: Verena Trenkel